# High-Reynolds-number simulation of turbulent mixing

P. K. Yeung[a] and D. A. Donzis
*School of Aerospace Engineering, Georgia Institute of Technology, Atlanta, Georgia 30332*

K. R. Sreenivasan
*International Centre for Theoretical Physics, Strada Costiera 11, 34014 Trieste, Italy*
*and Institute of Physical Science and Technology, University of Maryland, College Park, Maryland 20742*

(Received 12 May 2005; accepted 27 June 2005; published online 4 August 2005)

A brief report is given of a new $2048^3$ direct numerical simulation of the mixing of passive scalars with uniform mean gradients in forced, stationary isotropic turbulence. The Taylor-scale Reynolds number is close to 700 and Schmidt numbers of 1 and 1/8 are considered. The data provide the most convincing evidence to date for the inertial-convective scaling. Significant departures from small-scale isotropy are sustained in conventional measures. Subject to some stringent resolution requirements, the data suggest that commonly observed differences between the intermittency of energy and scalar dissipation rates may in part be a finite-Reynolds-number effect. © *2005 American Institute of Physics*. [DOI: 10.1063/1.2001690]

Recent advances in parallel computing power up to many teraflops in aggregate speed have created great opportunities for understanding the fundamental scaling properties of turbulence at adequately high Reynolds numbers. In particular, massive amounts of data from direct numerical simulations (DNS) are now available at grid resolutions $1024^3$ and above[1,2] with Reynolds numbers comparable to (and, in some cases, exceeding) those that laboratory experiments have often considered sufficiently high. The wide range of resolved scales in simulations has enabled the probing of various scaling issues with adequate precision and confidence. For example, simulations of Ref. 2 on a $4096^3$ grid, reaching a Taylor-scale Reynolds number $R_\lambda \approx 1200$, have provided new data on intermittency corrections to the energy spectrum in the inertial range while also confirming previous estimates of the Kolmogorov constant in experiments[3] and DNS.[1,4]

In this Letter, we present basic results from a $2048^3$ simulation aimed at addressing the fundamental aspects of mixing at high Reynolds number. Our simulation is based on the well-known algorithm of Rogallo,[5] which is Fourier pseudospectral in space and explicit, second order in time. Velocity and scalar fluctuations are maintained stationary, respectively, by the stochastic forcing scheme of Eswaran and Pope,[6] and by a uniform mean scalar gradient. (Comparison with DNS of isotropically forced scalar fields[7] would be of interest.) We used the resolution criterion $k_{\max}\eta = 1.5$ or better, where $k_{\max} = \sqrt{2}N/3$ is the highest wavenumber resolved on an $N^3$ grid and $\eta$ is the Kolmogorov length scale. Periodic boundary conditions are applied to the computational domain. Although idealized, this configuration is of great importance in the study of small-scale turbulence. The Schmidt number (Sc) is either 1 or 1/8, so the Kolmogorov scale is the limiting factor for resolution. Using about $2 \times 10^6$ CPU hours on 2048 of 6080 IBM SP processors at the Lawrence Berkeley National Laboratory NERSC facility, we have simulated the flow up to four eddy-turnover times although we report statistics mainly from the last two, when stationarity is better attained. Instantaneous velocity and scalar fields were archived at regular intervals for further analysis.

The averaged $R_\lambda$ for the flow thus simulated was just below 700. This Reynolds number is the highest known for the DNS of scalar mixing, and very close to the highest reported ($\sim$800) in related laboratory experiments.[8] Our emphasis here is on inertial-convective scaling expected for scalar mixing at high Reynolds number. The scaling is demonstrated in terms of the scalar spectrum and mixed structure functions. We also report on central issues of similarity scaling including departures from local isotropy in the presence of a mean gradient, and the intermittency of fluctuations of the scalar dissipation rate ($\chi$) compared to the energy dissipation ($\epsilon$).

As a demonstration of the quality of scaling in the velocity field, we show in Fig. 1 data for the "four-fifths law" of Kolmogorov,[9]

$$-\frac{\langle(\Delta_r u)^3\rangle}{\langle\epsilon\rangle r} = \frac{4}{5}, \tag{1}$$

where $\Delta_r u = u(x+r) - u(x)$ is the so-called longitudinal velocity increment (i.e., the velocity component and the separation distance are in the same direction). Equation (1) is an asymptotically exact result for the inertial range and its verification is the most stringent and direct criterion for the existence of a scaling region. We have included data at $R_\lambda \approx 240$ and 400 from $512^3$ and $1024^3$ simulations as well. As expected, the scaling region grows with the Reynolds number. While the present data at the highest $R_\lambda$ show good attainment of a "plateau" at 4/5, this is sensitive to temporal variability of the volume-averaged $\epsilon$ which, being driven by large scales, can vary by as much as 50% in our simulations even in a period of statistical stationarity.

Figure 2 shows the "compensated" scalar spectrum in

[a]Telephone: 1-404-894-9341. Fax: 1-404-894-2760. Electronic mail: pk.yeung@ae.gatech.edu

 

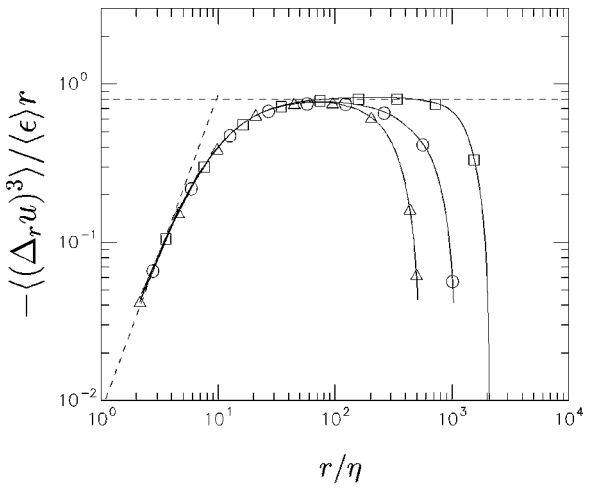


FIG. 1. The third-order velocity structure function scaled according to Kolmogorov's relation [see Eq. (1)] at $R_\lambda \approx 240$, 400, and 700 (triangles, circles, and squares, respectively). The dashed line of slope 2 gives the small $r$ asymptote $S/(15)^{3/2}(r/\eta)^2$ where $S \approx -0.5$ is the velocity gradient skewness.

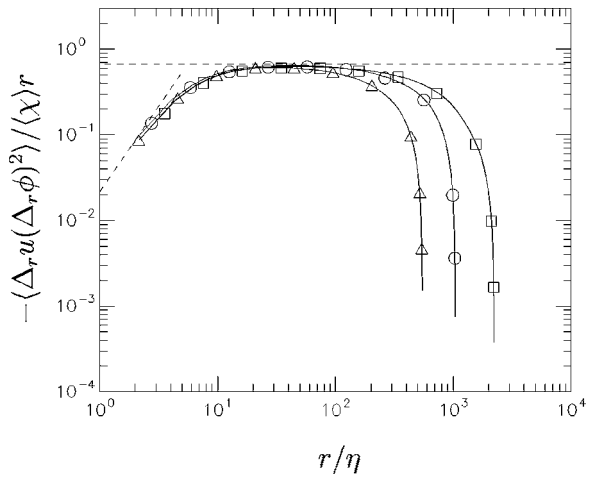


FIG. 3. Mixed velocity-scalar structure function scaled according to the Yaglom relation [see Eq. (3)] for Sc=1 at the same $R_\lambda$ as in Fig. 1. A dashed line of slope 2 gives the small $r$ asymptote [see Eq. (12) in Ref. 12].

the $2048^3$ simulation corresponding to the well-known inertial-convective range for wavenumbers[10,11] $1/L \ll k \ll 1/\eta_{OC} \leqslant 1/\eta$ (where $L$ is an integral length scale in the flow),

$$E_\phi(k) = C_\phi^* \langle\chi\rangle\langle\epsilon\rangle^{-1/3} k^{-5/3}, \tag{2}$$

$C_\phi^*$ being the Obukhov-Corrsin constant in the three-dimensional scalar spectrum function $E_\phi(k)$. This figure shows a better-developed scaling range for both Sc=1/8 and 1 compared to previous results at a lower Reynolds number.[12] For Sc=1 we also observe a spectral bump which is a consequence of viscous effects and may also be regarded[12] as the precursor to $k^{-1}$ Batchelor scaling that applies for high Sc. The height of the observed "plateau" is in excellent agreement with the value of $C_\phi^*$ inferred from experimental measurements[13] of the one-dimensional spectrum using spectral relations for an isotropic scalar field. [According to these relations, $C_\phi^*=0.67$ in $E_\phi(k)$ corresponds to the scaling constant of 0.4 in the one-dimensional spectrum.]

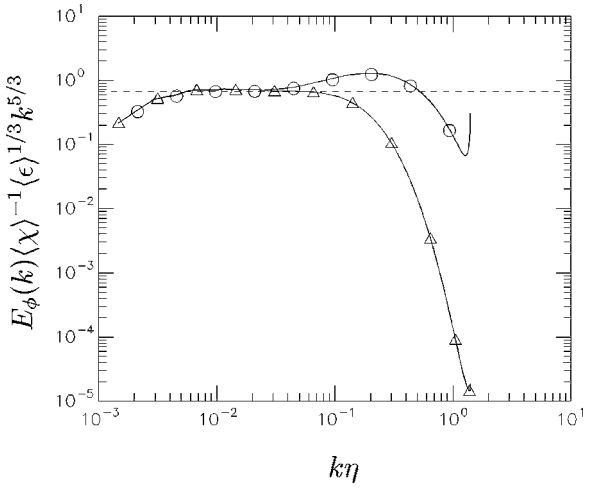


FIG. 2. Scalar spectrum according to Obukhov-Corrsin scaling in $2048^3$ DNS at $R_\lambda \approx 700$ and Sc=1/8 (triangles) and 1 (circles). The dashed line at 0.67 is for comparison with experiment (see Ref. 13).

In physical space the most important scaling result is the "Yaglom relation,"[14]

$$-\frac{\langle\Delta_r u(\Delta_r \phi)^2\rangle}{\langle\chi\rangle r} = \frac{2}{3}, \tag{3}$$

with the increments of velocity and the scalar taken over distances $\eta \ll r \ll L$, and the mean scalar dissipation rate defined as $\langle\chi\rangle = 2D\langle\nabla\phi\cdot\nabla\phi\rangle$. In our DNS there is some difference among results for $r$ taken in different directions because of anisotropy in the scalar field (see Ref. 12, and Fig. 5 therein) but we focus here on the component average as a basic measure. Figure 3 shows the normalized mixed structure function of Eq. (3), for Sc=1 at three Reynolds numbers as in Fig. 1. For small $r$ the data follow closely an $r^2$ line derived from the Taylor-series expansion of both $u$ and $\phi$ in space; for large $r$ there is a steep drop as the normalized quantity on the left-hand side of Eq. (3) tends to zero. At intermediate values of $r$, a plateau develops with increasing Reynolds number and approaches the theoretical value of 2/3. It is somewhat surprising, however, that the plateau does not widen as much between $1024^3$ and $2048^3$ as the difference between $512^3$ and $1024^3$ suggests. We tentatively attribute this effect to the anisotropy of the large-scale scalar field (see later). The width of the scaling range in Fig. 3 is restricted by the integral length scale of the scalar field which is smaller than that for the velocity. It is also for this reason that the scaling ranges in the velocity and scalar fields differ.

Figures 1–3 suggest that conditions suitable for addressing important scaling issues in turbulent mixing have been reached in our data. We noted that the large-scale anisotropy limits the scaling of the passive scalar. In fact, the anisotropy of the scalar field extends to dissipative scales.[15,16] In the present simulations (as in the experiments of Ref. 8) it is natural to compare the statistics of scalar gradients parallel and perpendicular to the imposed mean gradient, denoted by $\nabla_\parallel\phi$ and $\nabla_\perp\phi$ respectively. In particular, while odd-order moments of $\nabla_\perp\phi$ are indeed zero as required by reflectional symmetry, those of $\nabla_\parallel\phi$ are known to break this symmetry

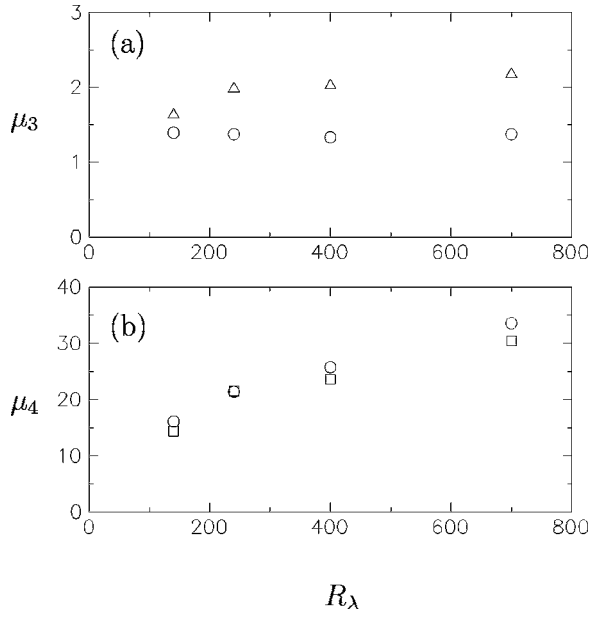


FIG. 4. Skewness ($\mu_3$) and flatness ($\mu_4$) factors of scalar gradient component fluctuations at different $R_\lambda$. $\nabla_\parallel \phi$ at Sc=1/8 (triangles), $\nabla_\parallel \phi$ at Sc=1 (circles), and $\nabla_\perp \phi$ at Sc=1 (squares).

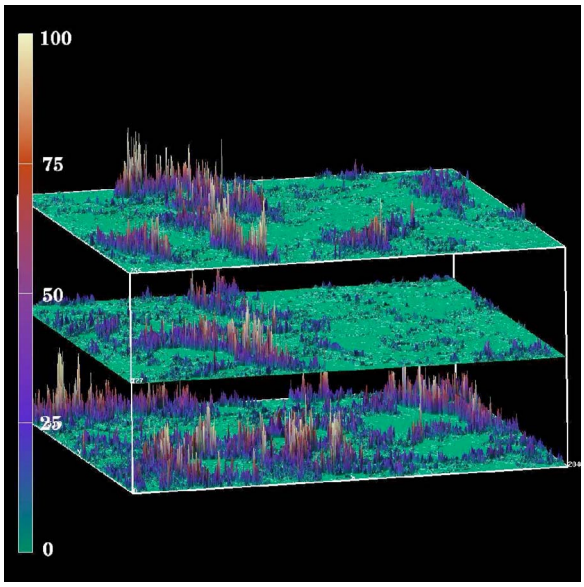


FIG. 5. (Color online). Spatial distribution of the scalar dissipation rate for Sc=1 shown as elevated surfaces for three chosen grid planes in the $2048^3$ simulation.

and deviate substantially from zero; at the same time, the flatness factors of both $\nabla_\parallel \phi$ and $\nabla_\perp \phi$ increase with the Reynolds number. We show the relevant skewness and flatness factors in Figs. 4(a) and 4(b). Consistent with the data of Refs. 3 and 8, the gradient skewness is of the order unity, confirming that some departure from local isotropy remains even at the highest Reynolds number reached here.

There have been suggestions in the literature[17] that relative constancy of a derivative skewness (as above) may not in itself be sufficient evidence for anisotropy at the small scales, in part because different normalization factors for the odd-order moments can lead to seemingly different conclusions. Additional information has been obtained in the spectral distribution of this skewness, which can be quantified by computing the cospectrum between a scalar gradient and its square, defined such that its integral in wavenumber space is equal to the third moment of the scalar gradient. We find that this quantity, called the skewness cospectrum,[18] possesses nontrivial values, including, for Sc=1, a local maximum at scales represented by $k\eta = O(0.1)$. This and other quantities such as the spectra of scalar gradient components indicate that, overall, the anisotropy originating at the large scales due to the mean gradient does percolate down to the smallest scales in the scalar field.

Many studies in the literature[19] suggest that, at the small scales, the scalar field is, by various measures, more intermittent than the velocity. To illustrate this, we show in Fig. 5 a visualization of the the instantaneous scalar dissipation $\chi$ in space in our $2048^3$ simulation, and in Fig. 6 the probability density functions (PDFs) of energy and scalar dissipation rates. The scalar dissipation shows localized zones of intense fluctuations with a sheet-like structure which is more readily revealed in the present rendering than two-dimensional contours in a previous work.[20] (The energy dissipation is, by contrast, more tube-like.) In Fig. 6 we have included data on the enstrophy, at the two Reynolds numbers of the $512^3$ and $2048^3$ simulations. In general, all of these PDFs have wide tails, indicating significant probability for fluctuations much larger than the mean value. At a given Reynolds number, the scalar dissipation has a wider tail than enstrophy, which itself has a wider tail than the energy dissipation. As the Reynolds number increases, the PDF of $\epsilon$ shows the greatest change,

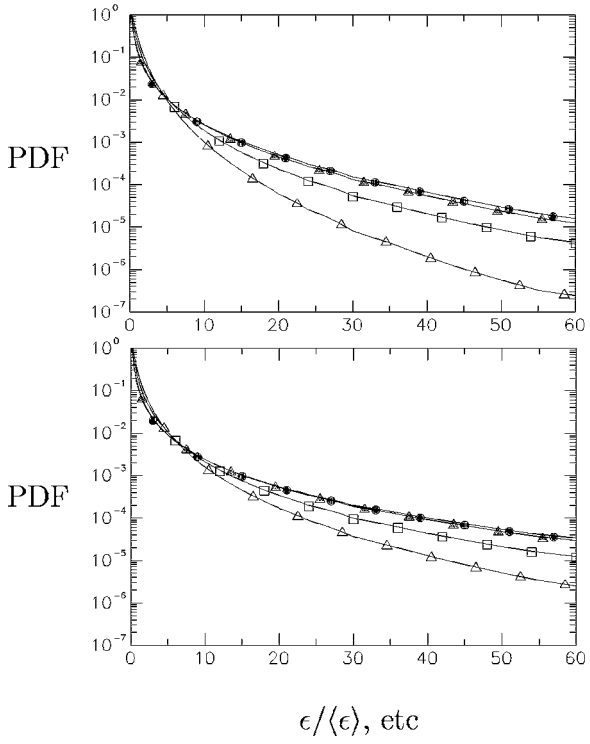


FIG. 6. PDFs of energy dissipation rate (△), enstrophy (□), and scalar dissipation rate at Sc=1/8 (▲) and 1 (●) from (top) $512^3$ DNS at $R_\lambda \approx 240$ and (bottom) $2048^3$ DNS at $R_\lambda \approx 700$. All variables are normalized by the mean.

whereas that of $\chi$ shows the least tendency to become flatter. This suggests that some of the differences among $\epsilon, \omega^2$, and $\chi$ are due to finite Reynolds number. The variances of $\ln \chi$ (which is important in modeling) estimated from the data are 3.33 and 3.73 for Sc=1/8 and 1 at $R_\lambda \approx 240$, and 4.39 and 4.29, respectively, at $R_\lambda \approx 700$. The last of these numbers is probably too low, which supports a recent assertion[21] that a higher degree of resolution (larger $k_{\max}\eta$) is required at a higher Reynolds number.

Our main purpose in this Letter has been to document a few primary characteristics of a new $2048^3$ DNS database which (together with previous data from $64^3$ to $1024^3$) potentially allows newer, and more definitive, physical insights into the subject of turbulent mixing at high Reynolds number. Our results show that an inertial-convective range has been achieved in both spectral and physical space, but that the small scales of the scalar remember the anisotropy of the large scale. The data also suggest that the PDFs of energy dissipation, enstrophy, and scalar dissipation may converge to the same shape at a high enough Reynolds number. Other quantitative aspects such as anomalous scaling, multifractal measures, and intermittency exponents, will be analyzed in detail and reported separately in the future.

We gratefully acknowledge support from the National Science Foundation, via Grants No. CTS-0121030 (P.K.Y.) and No. CTS-0121007 (K.R.S.), and via resources provided by the NPACI partnership at the San Diego Supercomputer Center. The present calculations were made possible largely by a U.S. Department of Energy Office of Science INCITE Award (December 2003) of supercomputer time at the NERSC facility, where we were assisted especially by Dr. David Skinner and Cristina Siergerist. Valuable comments by Professor R. A. Antonia and Professor R. W. Bilger are also much appreciated.

[1] T. Gotoh, D. Fukayama, and T. Nakano, "Velocity field statistics in homogeneous steady turbulence obtained using a high-resolution direct numerical simulation," Phys. Fluids **14**, 1065 (2002).
[2] Y. Kaneda, T. Ishihara, M. Yokokawa, K. Itakura, and A. Uno, "Energy dissipation rate and energy spectrum in high resolution direct numerical simulations of turbulence in a periodic box," Phys. Fluids **15**, L21 (2003).
[3] K. R. Sreenivasan, "On the universality of the Kolmogorov constant," Phys. Fluids **7**, 2778 (1995).
[4] P. K. Yeung and Y. Zhou, "On the universality of the Kolmogorov constant in numerical simulations of turbulence," Phys. Rev. E **56**, 1746 (1997).
[5] R. S. Rogallo, NASA Technical Memo 81315, 1981.
[6] V. Eswaran and S. B. Pope, "An examination of forcing in direct numerical simulations of turbulence," Comput. Fluids **16**, 257 (1988).
[7] T. Watanabe and T. Gotoh, "Statistics of a passive scalar in homogeneous turbulence," New J. Phys. **6**, 40 (2004).
[8] L. Mydlarski and Z. Warhaft, "Passive scalar statistics in high-Peclet-number grid turbulence," J. Fluid Mech. **358**, 135 (1998).
[9] A. N. Kolmogorov, "Dissipation of energy in locally isotropic turbulence," Dokl. Akad. Nauk SSSR **32**, 16 (1941); reprinted in English translation in Proc. R. Soc. London, Ser. A **434**, 15 (1991).
[10] A. M. Obukhov, "The structure of the temperature field in a turbulent flow," Izv. Akad. Nauk SSSR, Ser. Geogr. Geofiz. **13**, 58 (1949).
[11] S. Corrsin, "On the spectrum of isotropic temperature fluctuations in isotropic turbulence," J. Appl. Phys. **22**, 469 (1951).
[12] P. K. Yeung, S. Xu, and K. R. Sreenivasan, "Schmidt number effects on turbulent transport with uniform mean scalar gradient," Phys. Fluids **14**, 4178 (2002).
[13] K. R. Sreenivasan, "The passive scalar spectrum and the Obukhov-Corrsin constant," Phys. Fluids **8**, 189 (1996).
[14] A. M. Yaglom, "On the local structure of a temperature field in a turbulent flow," Dokl. Akad. Nauk SSSR **69**, 743 (1949).
[15] K. R. Sreenivasan, "On local isotropy of passive scalars in turbulent shear flows," Proc. R. Soc. London, Ser. A **434**, 165 (1991).
[16] Z. Warhaft, "Passive scalars in turbulent flows," Annu. Rev. Fluid Mech. **425**, 161 (2000).
[17] S. Kurien and K. R. Sreenivasan, "Measures of anisotropy and the universal properties of turbulence," in *New Trends in Turbulence*, NATO Advanced Study Institute, Les Houches (Springer and EDP-Sciences, New York, 2001), pp. 53–111.
[18] P. Mestayer, "Local isotropy and anisotropy in a high-Reynolds-number turbulent boundary layer," J. Fluid Mech. **125**, 475 (1982).
[19] K. R. Sreenivasan and R. A. Antonia, "The phenomenology of small-scale turbulence," Annu. Rev. Fluid Mech. **29**, 435 (1997).
[20] P. Vedula, P. K. Yeung, and R. O. Fox, "Dynamics of scalar dissipation in isotropic turbulence: a numerical and modelling study," J. Fluid Mech. **433**, 29 (2001).
[21] K. R. Sreenivasan, "Some aspects of scalar dissipation," Flow, Turbul. Combust. **72**, 93 (2004).